

## **Surface Evolution of Crystalline Tubes**

Fuqian Yang <sup>a</sup>, Wei Song <sup>b</sup> and Jun Zhang <sup>b</sup>

a) Department of Chemical and Materials Engineering

b) Department of Computer Science

University of Kentucky, Lexington, KY 40506

Technical Report No. 362-02, Department of Computer  
Science, University of Kentucky, KY, 2002

December 4, 2002

## Abstract

The surface evolution of an annular tube has been established on the basis of lattice diffusion and linear stability analysis. Without surface disturbance the annular tube will shrink to reduce the surface energy while the cross-sectional area of the tube remains constant. For an annular tube having infinitesimal thickness, the time dependence of the tube radius follows a linear law. When surface energy is significant, a new dispersion relation describing the morphological stability of crystalline tubes due to longitudinal surface perturbation has been formulated. A criterion has been obtained on the dependence of perturbation growth rate on perturbation frequency. The perturbation will grow when the perturbation frequency is less than the critical frequency, which is equal to the inverse of the inner surface radius. To our surprise, the critical frequency for an annular tube of infinitesimal thickness is the same as that given by Nichols and Mullins [Trans. Metall. Soc. AIME 233(1965) 1840] for an infinitely cylindrical rod. A finite spatial frequency for maximum growth rate was also obtained, which depends on the ratio of the inner surface radius to the outer surface radius. The surface instability will lead to the formation of closed end of crystalline tubes.

### 1. Introduction

The discovery of nanomaterials such as carbon nanotubes, nanowires has stimulated great interests in scientific community and industry. Due to the nanometer length scale, nanomaterials have displayed unique chemical and physical properties different from traditional materials with the micro-length scale. To understand the fundamental properties of nanomaterials including nanocrystals, nanotubes, and nanoparticles, different approaches by using atomic force microscope (AFM), nanoindentation, SEM, and TEM have been developed and used for characterizing the electrical, chemical, mechanical and other properties of nanomaterials. For examples, Paulson et al. [1] used the AFM to manipulate multi-walled nanotubes and found that changes in the sample resistance were small unless the nanotubes fractured or the metal-tube contact was perturbed. Tomblor et al. [2] studied the electromechanical characteristics of carbon nanotubes (CNTs) by using the AFM probe manipulation. Xie et al. [3] used SEM and TEM as well as Renishaw Raman microscope system to characterize the morphologies, distributions and microstructures of various CNTs formed on different substrates by chemical vapor deposition. Wang et al. [4] used in situ TEM to measure mechanical properties of individual CNTs.

The progresses in nanotechnology and nanoscience have led to the development of nano-electromechanical systems (NEMS), molecular diodes, switches, and other nano-electronic devices by using nanostructure of nanometer length scale. Lieber's group of MIT [5] proposed a concept of a carbon nanotube-based nonvolatile random access memory (RAM). Therefore the morphological stability of nanostructure such as nanotubes, nanowires, and nanoparticles used in nanodevices is becoming increasingly important as the linear size of these nanodevices decreases. It is necessary to investigate the morphological stability of nanomaterials in order to improve the reliability and performance of nanodevices.

The study of morphological stability has a long history in materials science. Representative of these studies is the one performed by Nichols and Mullins [6], in which, by using the linear perturbation analysis they considered the stability of an infinitely long cylinder and a cylindrical void in an infinite medium with isotropic surface energy. Considering surface and lattice diffusion, they determined the critical wavelength of perturbations at which the morphological instability occurs. Recently, nonlinear analysis [7] was performed to investigate the wavelength and perturbation growth rate variations when large fluctuation amplitudes were involved.

However, there is no study on the surface instability of annular tubes, which may provide insight on the long-term reliability of nanodevices and NEMS made from crystalline nanotubes.

In this paper, we examine the transverse growth behavior of annular tubes and the lateral surface instability of crystalline tubes by using the lattice diffusion theory and linear stability analysis. The transverse growth behavior of an annular tube is obtained if there is no surface disturbance. By introducing sinusoidal fluctuations along the surface of the annular tube, a new dispersion relationship describing the morphological growth of the annular tube is derived.

## 2. Shrinking Behavior of Annular Tubes

Consider a crystalline tube, whose morphological evolution is controlled by lattice diffusion. The concentration of vacancies ( $c$ ) in the nanotube follows the Laplace equation

$$\nabla^2 c = 0 \quad (1)$$

First assume that there is no perturbation along the surfaces of the tube and both the inner and outer surfaces are parallel to each other. The concentration of vacancies in the surfaces of the tube can be described by the Gibbs-Thomson equation [6, 8]

$$c = -\frac{\gamma\Omega K}{kT}c_0 + c_0 \quad (2)$$

which gives

$$c|_{r=r_o} = -\frac{\gamma\Omega c_0}{kT} \cdot \frac{1}{r_o} + c_0 \quad (3)$$

and

$$c|_{r=r_i} = \frac{\gamma\Omega c_0}{kT} \cdot \frac{1}{r_i} + c_0 \quad (4)$$

where  $\gamma$  is the specific surface energy per unit area,  $\Omega$  atomic volume,  $c_0$  the concentration of vacancies in equilibrium with a flat surface,  $k$  the Boltzmann constants,  $T$  the absolute temperature,  $K$  the mean surface curvature, and  $r_o$  and  $r_i$  the radii of the outer surface and inner surface of the annular tube respectively.

Let us introduce the following dimensionless variables,

$$\tilde{c} = \frac{c - c_0}{c_0} \quad \text{and} \quad \tilde{r} = \frac{r}{r_o} \quad (5)$$

Using the conditions of (3 and 4), axisymmetric and surface-perturbation free conditions, the vacancies concentration in the tube is

$$\tilde{c}(\tilde{r}) = \frac{\gamma\Omega}{kT} \left( \frac{1}{r_i} + \frac{1}{r_o} \right) \cdot \frac{\ln \tilde{r}}{\ln(r_i/r_o)} - \frac{\gamma\Omega}{kT} \cdot \frac{1}{r_o} \quad (6)$$

This gives the flux of vacancies normal to the surfaces of the tube as

$$J|_{\tilde{r}=1} = -D \frac{c_0 \partial \tilde{c}}{r_o \partial \tilde{r}} \Big|_{\tilde{r}=1} = -\frac{Dc_0\gamma\Omega}{kTr_o} \left( \frac{1}{r_i} + \frac{1}{r_o} \right) \cdot \frac{1}{\ln(r_i/r_o)} \quad (7)$$

$$J|_{\tilde{r}=\tilde{r}_i} = -D \frac{c_0 \partial \tilde{c}}{r_o \partial \tilde{r}} \Big|_{\tilde{r}=\tilde{r}_i} = -\frac{Dc_0\gamma\Omega}{kTr_i} \left( \frac{1}{r_i} + \frac{1}{r_o} \right) \cdot \frac{1}{\ln(r_i/r_o)} \quad (8)$$

Since the flux of vacancies is perpendicular to the surface of the tube, the average normal migration velocity of the surfaces is simply  $-\Omega J$ . Therefore,

$$\frac{dr_o}{dt} = -\Omega J|_{\bar{r}=1} = \frac{Dc_0\gamma\Omega^2}{kTr_o} \left( \frac{1}{r_i} + \frac{1}{r_o} \right) \cdot \frac{1}{\ln(r_i/r_o)} \quad (9)$$

$$\frac{dr_i}{dt} = -\Omega J|_{\bar{r}=\bar{i}} = \frac{Dc_0\gamma\Omega^2}{kTr_i} \left( \frac{1}{r_i} + \frac{1}{r_o} \right) \cdot \frac{1}{\ln(r_i/r_o)} \quad (10)$$

Obviously, the tube will shrink to reduce the system energy ( $\ln(r_i/r_o) < 0$ ). From equations (9 and 10), we have

$$r_o^2(t) - r_i^2(t) \equiv a^2 = \text{constant} \quad (11)$$

The cross-sectional area of the annular tube remains constant during the shrinkage of the tube. Substituting Eq. (11) into Eqs. (9 and 10), the shrinkage behavior of both the outer-surface and inner surface radii of the tube are

$$t = \frac{kT}{Dc_0\gamma\Omega^2} \int_{r_o(0)}^{r_o(t)} \frac{r^2 \sqrt{r^2 - a^2} \ln(\sqrt{r^2 - a^2}/r)}{r + \sqrt{r^2 - a^2}} dr \quad (12)$$

$$t = \frac{kT}{Dc_0\gamma\Omega^2} \int_{r_i(0)}^{r_i(t)} \frac{r^2 \sqrt{r^2 + a^2} \ln(r/\sqrt{r^2 + a^2})}{r + \sqrt{r^2 + a^2}} dr \quad (13)$$

Figure 1 shows the time dependence of the out-surface radius of the tube. The radius of the tube shrinks with time. For large cross-sectional area of tubes, the shrink rate is less than that with small area, which is due to the larger migration distance for vacancies diffusing from the inner surface to the outer surface.

Now consider the limiting case  $r_o - r_i \ll r_i < r_o$ , Eq. (11) gives

$$\frac{r_o(t) - r_i(t)}{r_o(t)} = \frac{a^2}{r_o(r_o + r_i)} \approx a^2 / 2r_o^2 \ll 1 \quad (14)$$

Using the condition  $r_o(t) \approx r_i(t)$  and Eq. (14), Eq. (9) can be reduced to

$$\frac{dr_o}{dt} = -\frac{4Dc_0\gamma\Omega^2}{kTa^2} \quad (15)$$

which gives

$$r_o(t) = r_o(0) - \frac{4Dc_0\gamma\Omega^2}{kTa^2} t \quad (16)$$

A linear shrinkage behavior for an annular tube with an infinitesimal thickness is obtained. The shrinkage rate is inversely proportional to the temperature and the cross-sectional area of the tube.

### 3. Morphological Instability of Crystalline Tubes – Linear Stability Analysis

#### a) Longitudinal Perturbations

Now consider the surface instability of the crystalline tube under small surface perturbations as shown in Fig. 2. Based on the small slope approximation, the mean surface curvature of the crystalline tube under axisymmetric surface disturbance can be expressed as

$$K|_{r=r_o} = \frac{1}{r} - \frac{d^2r}{dz^2} \quad (17)$$

$$K|_{r=r_i} = -\frac{1}{r} + \frac{d^2r}{dz^2} \quad (18)$$

Introduce infinitesimal longitudinal sinusoidal perturbations in the shape of the cylindrical surface in which the surface evolution is axisymmetric. The equations of the perturbed surfaces are then given by

$$r_{outer\ surface} = r_o + \delta_o \sin(\omega z) \quad (19)$$

$$r_{inner\ surface} = r_i + \delta_i \sin(\omega z + \varphi) \quad (20)$$

where  $\delta_o$  and  $\delta_i$  are the amplitudes of the surface perturbations at the outer and inner surfaces respectively,  $\omega$  is the spatial frequency, and  $\varphi$  is the phase difference between the outer and inner surface perturbations. Thus the concentrations of vacancies at both the outer and the inner surfaces correct to the first order terms in  $\delta_o$  and  $\delta_i$  can be expressed as

$$c|_{r=r_o} = -\frac{\gamma\Omega c_0}{kT} [r_o^{-1} - (r_o^{-2} - \omega^2)\delta_o \sin(\omega z)] + c_0 \quad (21)$$

$$c|_{r=r_i} = \frac{\gamma\Omega c_0}{kT} [r_i^{-1} - (r_i^{-2} - \omega^2)\delta_i \sin(\omega z + \varphi)] + c_0 \quad (22)$$

Using the symmetrical condition, the solution of Eq. (1) in the cylindrical coordinate is

$$\tilde{c} = [AI_0(\omega r) + BK_0(\omega r)][C \sin(\omega z) + D \cos(\omega z)] + \frac{\gamma\Omega}{kT} \left( \frac{1}{r_i} + \frac{1}{r_o} \right) \cdot \frac{\ln \tilde{r}}{\ln(r_i/r_o)} - \frac{\gamma\Omega}{kT} \cdot \frac{1}{r_o} \quad (23)$$

where  $A$ ,  $B$ ,  $C$ , and  $D$  are constants to be determined,  $I_0(\omega r)$  and  $K_0(\omega r)$  are the first and second modified Bessel functions of order zero respectively. There are four constants in Eq. (23) to be determined, while there are only two equations of (21 and 22) available as boundary conditions. Thus, it requires  $D = 0$  and  $\varphi = 0$ , and Eq. (23) reduces to

$$\tilde{c} = [AI_0(\omega r) + BK_0(\omega r)] \sin(\omega z) + \frac{\gamma\Omega}{kT} \left( \frac{1}{r_i} + \frac{1}{r_o} \right) \cdot \frac{\ln(r/r_o)}{\ln(r_i/r_o)} - \frac{\gamma\Omega}{kT} \cdot \frac{1}{r_o} \quad (24)$$

Using the boundary conditions (21 and 22), the vacancies concentration in the tube is

$$\tilde{c}(r) = \frac{\gamma\Omega}{kT} \frac{g(\omega, r_o, r)(1 - r_i^2 \omega^2) r_o^2 \delta_i + g(\omega, r_i, r)(1 - r_o^2 \omega^2) r_i^2 \delta_o}{r_o^2 r_i^2 g(\omega, r_i, r_o)} \sin(\omega z) \quad (25)$$

$$+ \frac{\gamma\Omega}{kT} \left( \frac{1}{r_i} + \frac{1}{r_o} \right) \cdot \frac{\ln(r/r_o)}{\ln(r_i/r_o)} - \frac{\gamma\Omega}{kT} \cdot \frac{1}{r_o}$$

where

$$g(\omega, x, y) = I_0(\omega x)K_0(\omega y) - I_0(\omega y)K_0(\omega x) \quad (26)$$

The second term on the right side of Eq. (25) is related to the shrinkage of the tube, which has been discussed in the previous section. To analyze the morphological instability, we only focus on the first term on the right side of Eq. (25). Using Eq. (25), the flux of vacancies normal to the surfaces of the tube due to the surface perturbation is then given by Fick's first law as

$$J|_{r=r_o} = -D \frac{\partial c}{\partial r} \Big|_{r=r_o} = \frac{Dc_0 \gamma\Omega}{kT} \cdot \frac{r_i^2 (1 - r_o^2 \omega^2) \delta_o u(\omega, r_o, r_i) + r_o^2 (1 - r_i^2 \omega^2) \delta_i u(\omega, r_o, r_o)}{r_o^2 r_i^2 g(\omega, r_i, r_o)} \omega \sin(\omega z) \quad (27)$$

$$J|_{r=r_i} = -D \frac{\partial c}{\partial r} \Big|_{r=r_i} = \frac{Dc_0 \gamma\Omega}{kT} \cdot \frac{r_i^2 (1 - r_o^2 \omega^2) \delta_o u(\omega, r_i, r_i) + r_o^2 (1 - r_i^2 \omega^2) \delta_i u(\omega, r_i, r_o)}{r_o^2 r_i^2 g(\omega, r_i, r_o)} \omega \sin(\omega z) \quad (28)$$

where  $u(\omega, x, y) = I_1(\omega x)K_0(\omega y) + I_0(\omega y)K_1(\omega x)$ ,  $I_1(\omega r)$  and  $K_1(\omega r)$  are the first and second modified Bessel functions of order one respectively. Since the flux of vacancies is perpendicular to the surface of the tube, the average growth velocity of the surfaces is simply  $-\Omega J$ . The surface growth rates induced by the surface perturbations are

$$\left. \frac{dr}{dt} \right|_{r=r_o} = -\Omega J \Big|_{r=r_o} = -\frac{Dc_0\gamma\Omega^2}{kT} \frac{r_i^2(1-r_o^2\omega^2)\delta_0 u(\omega, r_o, r_i) + r_o^2(1-r_i^2\omega^2)\delta_i u(\omega, r_o, r_o)}{r_o^2 r_i^2 g(\omega, r_i, r_o)} \omega \sin(\omega z) \quad (29)$$

$$\left. \frac{dr}{dt} \right|_{r=r_i} = -\Omega J \Big|_{r=r_i} = -\frac{Dc_0\gamma\Omega^2}{kT} \frac{r_i^2(1-r_o^2\omega^2)\delta_0 u(\omega, r_i, r_i) + r_o^2(1-r_i^2\omega^2)\delta_i u(\omega, r_i, r_o)}{r_o^2 r_i^2 g(\omega, r_i, r_o)} \omega \sin(\omega z) \quad (30)$$

Using Eqs. (19 and 20) and  $\phi = 0$ , we have

$$\left. \frac{dr}{dt} \right|_{r=r_o} = \sin(\omega z) \frac{d\delta_o}{dt} \quad \text{and} \quad \left. \frac{dr}{dt} \right|_{r=r_i} = \sin(\omega z) \frac{d\delta_i}{dt} \quad (31)$$

in which only the surface growth due to the surface perturbations is considered. Comparing Eq. (31) to Eqs. (29 and 30), there are

$$\frac{d\delta_o}{dt} = -\frac{\omega Dc_0\gamma\Omega^2}{kT} \frac{r_i^2(1-r_o^2\omega^2)\delta_0 u(\omega, r_o, r_i) + r_o^2(1-r_i^2\omega^2)\delta_i u(\omega, r_o, r_o)}{r_o^2 r_i^2 g(\omega, r_i, r_o)} \quad (32)$$

$$\frac{d\delta_i}{dt} = -\frac{\omega Dc_0\gamma\Omega^2}{kT} \frac{r_i^2(1-r_o^2\omega^2)\delta_0 u(\omega, r_i, r_i) + r_o^2(1-r_i^2\omega^2)\delta_i u(\omega, r_i, r_o)}{r_o^2 r_i^2 g(\omega, r_i, r_o)} \quad (33)$$

Both the outer and inner surface growth rates are a linear function of the surface perturbations. From Eqs. (32 and 33), the dispersion relation of the fractional rates for various frequencies of perturbations is

$$\frac{d^2\delta}{dt^2} + \alpha(A+D) \frac{d\delta}{dt} - \alpha^2(BC-AD)\delta = 0 \quad (34)$$

where  $\delta = \delta_i$  or  $\delta_o$ , and

$$\alpha = \frac{\omega Dc_0\gamma\Omega^2}{kT}$$

$$A = \frac{r_i^2(1-r_o^2\omega^2)u(\omega, r_o, r_i)}{r_o^2 r_i^2 g(\omega, r_i, r_o)}, \quad B = \frac{r_o^2(1-r_i^2\omega^2)u(\omega, r_o, r_o)}{r_o^2 r_i^2 g(\omega, r_i, r_o)}$$

$$C = \frac{r_i^2(1-r_o^2\omega^2)u(\omega, r_i, r_i)}{r_o^2 r_i^2 g(\omega, r_i, r_o)}, \quad D = \frac{r_o^2(1-r_i^2\omega^2)u(\omega, r_i, r_o)}{r_o^2 r_i^2 g(\omega, r_i, r_o)}$$

The growth behavior of the surface perturbations with the stable solution is

$$\delta = C_1 \cdot \exp\left(\frac{-\alpha(A+D) + \alpha\sqrt{(A+D)^2 + 4(BC-AD)}}{2} t\right) + C_2 \cdot \exp\left(\frac{-\alpha(A+D) - \alpha\sqrt{(A+D)^2 + 4(BC-AD)}}{2} t\right) \quad (35)$$

where  $C_1$  and  $C_2$  are two constants determined by the initial surface perturbation at the inner and outer surfaces and the spatial frequency of the surface perturbations.

The critical perturbation frequency for zero growth rate of the surface disturbances is then determined by the roots of the following two equations

$$\alpha[(A + D) - \sqrt{(A + D)^2 + 4(BC - AD)}] = 0 \quad (36)$$

$$\alpha[(A + D) + \sqrt{(A + D)^2 + 4(BC - AD)}] = 0 \quad (37)$$

which gives

$$f(\omega, r_o, r_i) \equiv \omega[f_1(\omega, r_o, r_i) - \sqrt{f_1^2(\omega, r_o, r_i) + 4f_2(\omega, r_o, r_i)}] = 0 \quad (38)$$

$$h(\omega, r_o, r_i) \equiv \omega[f_1(\omega, r_o, r_i) + \sqrt{f_1^2(\omega, r_o, r_i) + 4f_2(\omega, r_o, r_i)}] = 0 \quad (39)$$

where

$$f_1(\omega, r_o, r_i) = r_i^2(1 - r_o^2\omega^2)u(\omega, r_o, r_i) + r_o^2(1 - r_i^2\omega^2)u(\omega, r_i, r_o) \quad (40)$$

$$f_2(\omega, r_o, r_i) = r_i^2r_o^2(1 - r_i^2\omega^2)(1 - r_o^2\omega^2)[u(\omega, r_i, r_i)u(\omega, r_o, r_o) - u(\omega, r_o, r_i)u(\omega, r_i, r_o)] \quad (41)$$

Figure 3 shows the effect of the spatial frequency on the functions  $f(\omega, r_o, r_i)$  and  $h(\omega, r_o, r_i)$ .

Both the functions first increase with the spatial frequency and reach the maximum, then they decrease with the spatial frequency and become negative. The critical perturbation frequency for the zero growth rate is then determined by the maximum root of Eqs. (38 and 39). The roots of Eqs. (38 and 39) as a function of the spatial frequency are  $1/r_o$  and  $1/r_i$  respectively and are depicted in Fig. 4. The root of Eq. (39) is always larger than that for Eq. (38), while it decreases with the radius of the inner surface. Thus, the critical spatial frequency for the zero growth rate is

$$\omega_c = 1/r_i \quad (42)$$

The critical frequency is inversely proportional to the inner radius, which is the same as for an infinite cylindrical void in an infinite medium. To our surprise, the critical frequency for an annular tube of infinitesimal thickness is the same as that given by Nichols and Mullins [6] for an infinitely cylindrical rod,  $\omega_c = 1/r_o$ , which gives the critical wavelength  $\lambda_c = 2\pi/\omega_c = 2\pi r_o$ . Once the frequency of the surface perturbations is less than the critical frequency, the amplitude of the perturbations will spontaneously increase with time until the annular tube breaks up into a line of spherical shell.

To obtain the maximum growth rate, differentiate  $f(\omega, r_o, r_i)/|g(\omega, r_o, r_i)|$  and  $h(\omega, r_o, r_i)/|g(\omega, r_o, r_i)|$  respect with to  $\omega$  and equate the results to zero,

$$\left. \frac{\partial}{\partial \omega} \frac{f(\omega, r_o, r_i)}{|g(\omega, r_o, r_i)|} \right|_{r_o, r_i} = \left. \frac{\partial}{\partial \omega} \frac{h(\omega, r_o, r_i)}{|g(\omega, r_o, r_i)|} \right|_{r_o, r_i} = 0 \quad (43)$$

Numerical calculation is used to obtain the effect of the ratio  $r_i/r_o$  on the perturbation frequency of the maximum growth rate, which is shown in Fig. 5. There are two local maximum growth rates as expected from Fig 3. The frequency for the maximum growth rate of the branch  $f(\omega, r_o, r_i)/|g(\omega, r_o, r_i)|$  starts at  $\omega_{\max}r_o = 0.694$  for  $r_i/r_o \rightarrow 0$  and increases with the ratio. Then it reaches the maximum of  $\omega_{\max}r_o = 0.734$  at  $r_i/r_o = 0.83$  and decreases with the ratio. When  $r_i/r_o \rightarrow 1$ , the frequency approaches  $0.71/r_o$ , which gives the wavelength of the maximum growth rate  $8.85r_o$  - the same as that of the maximum instability of an infinite cylinder controlled by surface diffusion [6]. When  $r_i/r_o \rightarrow 0$ , the wavelength of the maximum instability for the branch  $f(\omega, r_o, r_i)/|g(\omega, r_o, r_i)|$  approaches  $9.05r_o$  - in agreement with that of the maximum

instability of an infinite cylinder controlled by lattice diffusion [6]. For the branch  $h(\omega, r_o, r_i) / |g(\omega, r_o, r_i)|$ , there exists nonzero frequency of the maximum instability only when  $r_i / r_o$  is less than 0.265, while the frequency of the maximum instability decreases with the ratio  $r_i / r_o$ . Figure 6 shows the maximum value of both functions  $f(\omega, r_o, r_i) / |g(\omega, r_o, r_i)|$  and  $h(\omega, r_o, r_i) / |g(\omega, r_o, r_i)|$  versus the ratio  $r_i / r_o$ . The local maximum decreases with the ratio  $r_i / r_o$ , while the maximum of the function  $h(\omega, r_o, r_i) / |g(\omega, r_o, r_i)|$  is much larger than that of the function  $f(\omega, r_o, r_i) / |g(\omega, r_o, r_i)|$ . This suggests that the morphological instability of a crystalline tube is controlled by the behavior of the function of  $h(\omega, r_o, r_i) / |g(\omega, r_o, r_i)|$ . Comparing to the cylindrical wire/rod, the tube is less stable.

### b) Circumferential Perturbations

Now consider circumferential perturbations having the following forms

$$r_{outer\ surface} = r_o + \delta_0 \sin(n\theta) \quad (44)$$

$$r_{inner\ surface} = r_i + \delta_i \sin(n\theta + \phi) \quad (45)$$

where  $n = 0, 1, 2, 3 \dots$ ,  $n$  is the angular frequency, and  $\phi$  is the phase difference between the outer and inner surface perturbations. For  $n = 0$ , there is no distortion; for  $n = 1$ , the tube is simply rotated. The first surface perturbation occurs at  $n = 2$ . Under the above surface disturbance, the surface evolution is not axisymmetric and independent of coordinate  $z$ . The mean curvature of the annular tube surfaces can be calculated as follow

$$K|_{outer\ surface} = \frac{1}{r} - \frac{1}{r^2} \frac{d^2 r}{d\theta^2} \quad (46)$$

$$K|_{inner\ surface} = -\frac{1}{r} + \frac{1}{r^2} \frac{d^2 r}{d\theta^2} \quad (47)$$

which give the concentration of vacancies on both surfaces of the tube as

$$c|_{outer\ surface} = -\frac{\gamma\Omega c_0}{kT} \left[ \frac{1}{r_o} + \frac{n^2 - 1}{r_o^2} \delta_0 \sin(n\theta) \right] + c_0 \quad (48)$$

$$c|_{inner\ surface} = \frac{\gamma\Omega c_0}{kT} \left[ \frac{1}{r_i} + \frac{n^2 - 1}{r_i^2} \delta_i \sin(n\theta + \phi) \right] + c_0 \quad (49)$$

The concentration of vacancies in the tube can be expressed as

$$\tilde{c} = [A'r^n + B'r^{-n}] [C'\sin(n\theta) + D'\cos(n\theta)] + \frac{\gamma\Omega}{kT} \left( \frac{1}{r_i} + \frac{1}{r_o} \right) \cdot \frac{\ln \tilde{r}}{\ln(r_i / r_o)} - \frac{\gamma\Omega}{kT} \cdot \frac{1}{r_o} \quad (50)$$

where  $A'$ ,  $B'$ ,  $C'$  and  $D'$  are to be determined. Based on the boundary conditions of Eq. (48 and 49), it requires  $D' = 0$  and  $\phi = 0$ , and Eq. (50) reduces to

$$\tilde{c} = [A'r^n + B'r^{-n}] \sin(n\theta) + \frac{\gamma\Omega}{kT} \left( \frac{1}{r_i} + \frac{1}{r_o} \right) \cdot \frac{\ln \tilde{r}}{\ln(r_i / r_o)} - \frac{\gamma\Omega}{kT} \cdot \frac{1}{r_o} \quad (51)$$

The vacancies concentration in the tube satisfying the boundary conditions of Eq. (48 and 49) is

$$\tilde{c} = -\frac{\gamma\Omega(n^2 - 1)}{kT} \frac{(r_o^n r_i^2 \delta_0 + r_o^2 r_i^n \delta_i) r^n - r_o^n r_i^n (r_i^{2+n} \delta_0 + r_o^{2+n} \delta_i) r^{-n}}{r_o^2 r_i^2 (r_o^{2n} - r_i^{2n})} \sin(n\theta) \quad (52)$$

$$+ \frac{\gamma\Omega}{kT} \left( \frac{1}{r_i} + \frac{1}{r_o} \right) \cdot \frac{\ln \tilde{r}}{\ln(r_i/r_o)} - \frac{\gamma\Omega}{kT} \cdot \frac{1}{r_o}$$

Using the same procedure, there are

$$\frac{d\delta_o}{dt} = - \frac{Dc_0\gamma\Omega^2}{kT} \frac{n(n^2-1)[r_i^2 r_o^{-1}(r_o^{2n} + r_i^{2n})\delta_0 + 2r_o^{1+n}r_i^n\delta_i]}{r_o^2 r_i^2 (r_o^{2n} - r_i^{2n})} \quad (53)$$

$$\frac{d\delta_i}{dt} = - \frac{Dc_0\gamma\Omega^2}{kT} \frac{n(n^2-1)[2r_o^n r_i^{1+n}\delta_0 + r_i^{-1}r_o^2(r_o^{2n} + r_i^{2n})\delta_i]}{r_o^2 r_i^2 (r_o^{2n} - r_i^{2n})} \quad (54)$$

In contrast to the case of longitudinal perturbations, the growth rate of the perturbation as shown in Eqs. (53 and 54) is determined by  $-n(n^2-1)$  and is negative for  $n \geq 2$ . The annular tube is stable to all circumferential perturbations.

#### 4. Discussion and Conclusions

In analyzing the surface evolution of an annular tube controlled by lattice diffusion, we have used the small slope approximation in the calculation of the mean surface curvature. By exactly solving the diffusion equation, we found that the cross-sectional area remains constant during the shrinkage and the annular tube size decreases with time to reduce the surface energy of the tube. For a tube with infinitesimal thickness, the shrinkage rate is proportional to time and inversely proportional to the cross-sectional area of the tube. A new quadratic dispersion relationship for the growth rate of the longitudinal surface perturbation along the surface of the tube has been established, which is different from the classical results given by Nichols and Mullins [6]. For the longitudinal perturbation, the perturbation will grow provided that the spatial frequency of the perturbation is less than the inverse of the inner surface radius. It is interesting to observe that the critical frequency for an annular tube of infinitesimal thickness is the same as that given by Nichols and Mullins [6] for an infinitely cylindrical rod. The tube is less stable than cylindrical rod/void. For longitudinal surface perturbation with spatial frequency less than the critical frequency, the tube will break up and form closed ends. However the circumferential disturbance will not introduce the morphological instability of annular tubes.

While the analysis is useful in determining the critical condition on the morphological instability of annular tubes such as nanotubes resulting from various surface perturbations, it is important to note that the size of annular tubes is time dependent controlled by kinetics. The appearance of a finite frequency for the maximum perturbation growth rate as shown in Fig. 5 depends on the ratio of the inner radius to the outer radius, which is time dependent. Thus the critical spatial frequency and the finite frequency for the maximum perturbation growth rate become a function of time. If the interaction between the outer and inner surfaces is negligible, the results for cylindrical rod and cylindrical void can be approximately used to estimate the critical frequency and the finite frequency for the maximum growth rate. The present results explain the role and influence of lattice diffusion on the surface instability of annular tubes. A non-linear analysis taking account of high order effect on the mean surface curvature and surface interaction will be interested in obtaining a more complete surface evolution of annular tubes.

#### References:

1. S. Paulson, M. R. Falvo, N. Snider, A. Helser, T. Hudson, A. Seeger, R. M. Taylor, R. Superfine, and S. Washburn, *Appl. Phys. Lett.* 75(1999) 2936-2938
2. T.W. Tomblor, C.W. Zhou, L. Alexseyev, J. Kong, H.J. Dai, L. Lei, C.S. Jayanthi, M.J. Tang, and S.Y. Wu, *Nature* 405(2000) 769-772

3. S.S. Xie, W.Z. Li, Z.W. Pan, B.H. Chang, and L.F. Sun, J. Phys. Chem. Solids 61(2000) 1153-1158
4. Z.L. Wang, P. Poncharal, and W.A. de Heer, J. Phys. Chem. Solids 61(2000) 1025-1030
5. T.W. Odom, J.L. Huang, and C.M. Lieber, Ann. NY Acad. Sci. 960(2002) 203-215
6. F.A. Nichols and W.W. Mullins, Trans. Metall. Soc. AIME 233(1965) 1840-1848
7. J.H. Choy, S.A. Hackney, and J.K. Lee, J. Appl. Phys. 77(1995) 5647-5654
8. Fuqian Yang, Comp. Mater. Sci. 7(1997) 279-284

**Figure captions:**

1. Growth behavior of a crystalline tube
2. A crystalline tube of diameter  $2r_0$  and thickness  $(r_o - r_i)$  subject to surface fluctuation
3. The dependence of the functions  $f(\omega, r_o, r_i)$  and  $h(\omega, r_o, r_i)$  on the spatial frequency
4. Dependence of the solution of Eq. (38 and 39) as a function of the ratio of the outer surface radius to the inner surface radius
5. Dependence of the frequency of the local maximum growth rate on the ratio  $r_i / r_o$
6. Dependence of the local maximum growth rate on the ratio  $r_i / r_o$

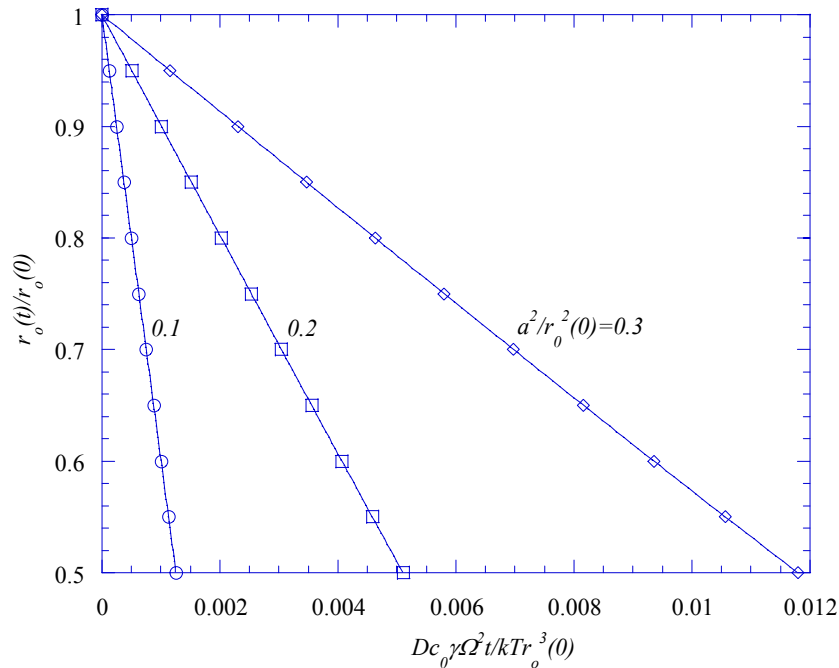


Figure 1. Growth behavior of a crystalline tube

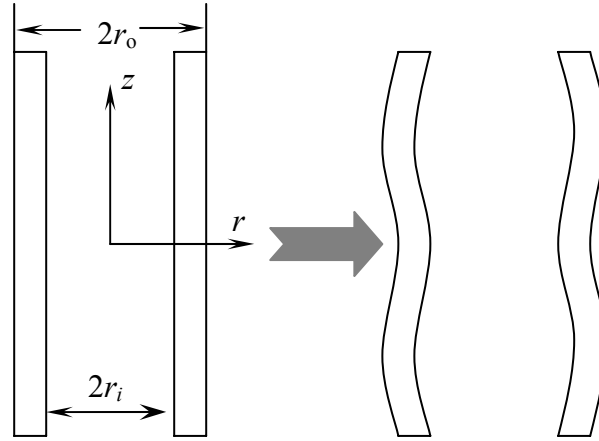


Figure 2. A crystalline tube of diameter  $2r_o$  and thickness  $(r_o - r_i)$  subject to surface fluctuation

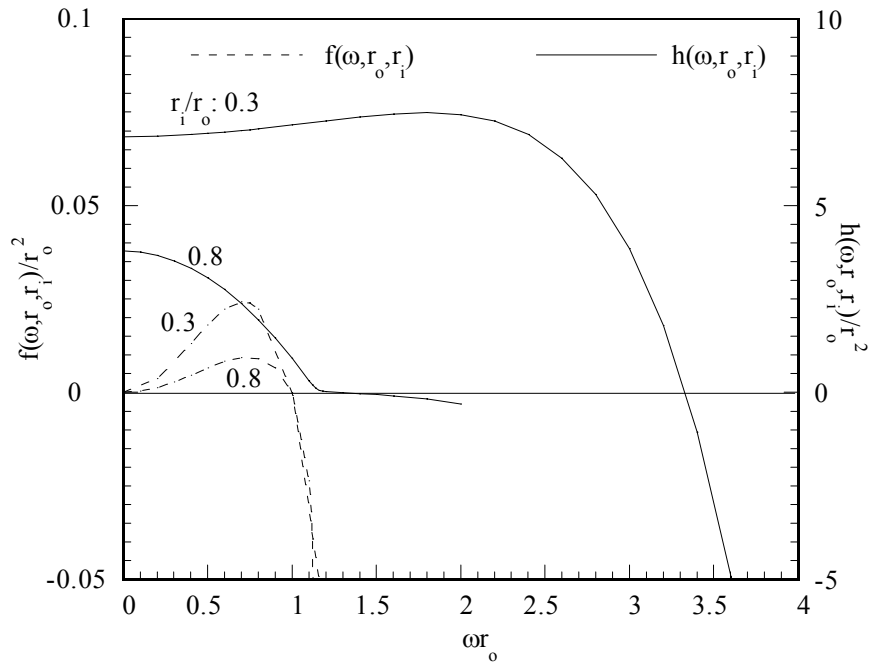


Figure 3. The dependence of the functions  $f(\omega, r_o, r_i)$  and  $g(\omega, r_o, r_i)$  on the spatial frequency

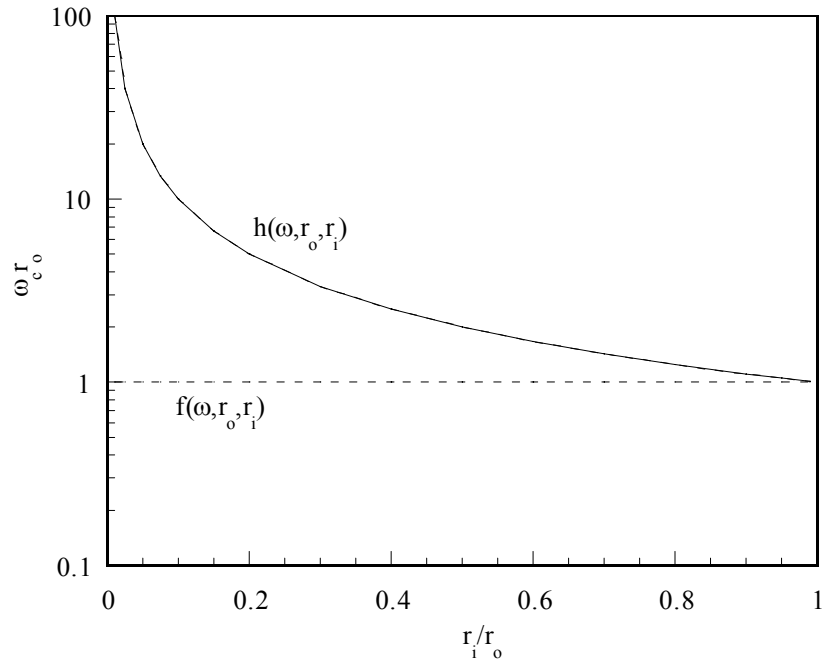


Figure 4. Dependence of the solution of Eq. (38 and 39) as a function of the ratio of the outer surface radius to the inner surface radius

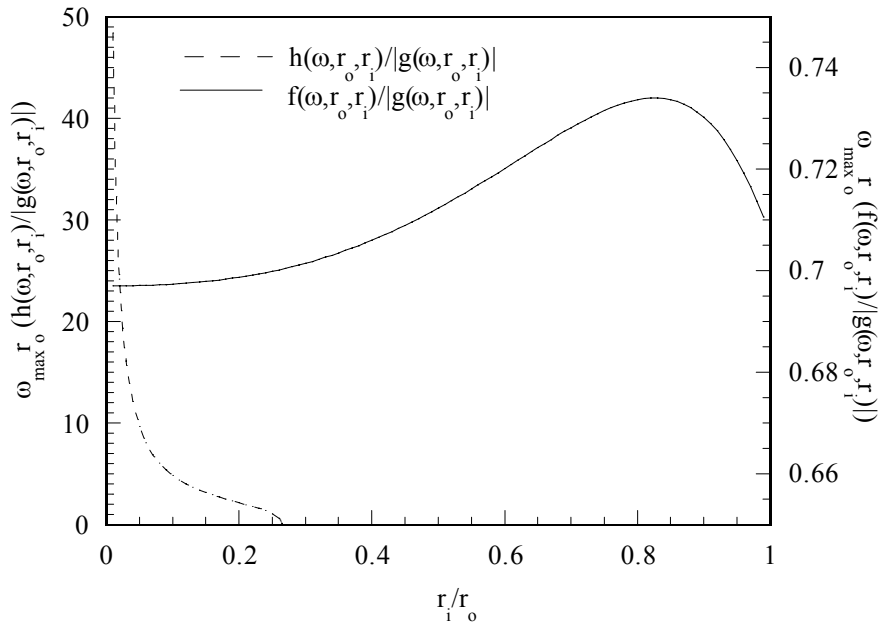


Figure 5. Dependence of the frequency of the local maximum growth rate on the ratio  $r_i/r_o$

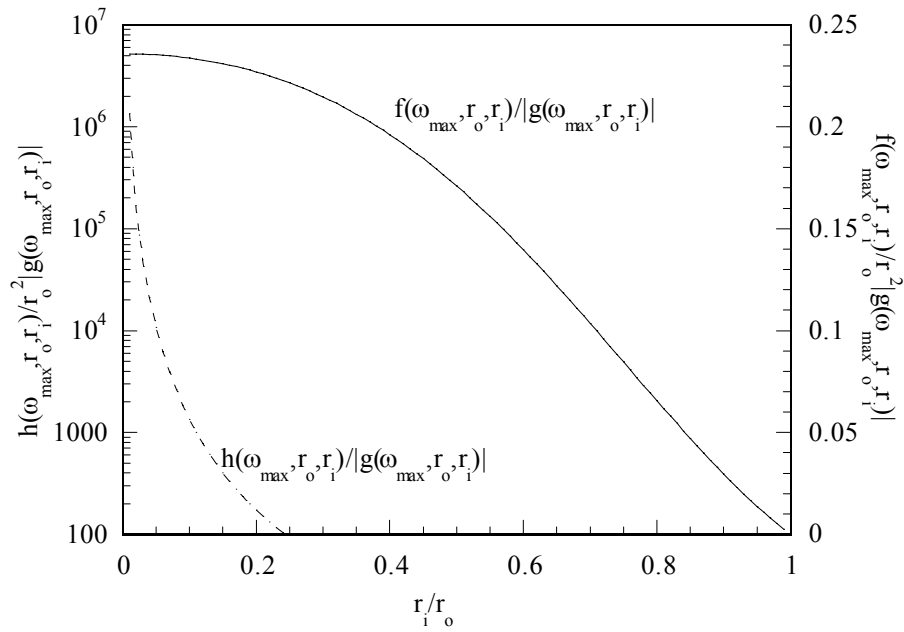


Figure 6. Dependence of the local maximum growth rate on the ratio  $r_i/r_o$